Prediction of the intestinal resistome by a three-dimensional structure-based method

Ruppé, Etienne; Ghozlane, Amine; Tap, Julien; Pons, Nicolas; Alvarez, Anne-Sophie; Maziers, Nicolas; Cuesta, Trinidad; Hernando-Amado, Sara; Clares, Irene; Martínez, Jose Luís; Coque, Teresa M; Baquero, Fernando; Lanza, Val F; Máiz, Luis; Goulenok, Tiphaine; de Lastours, Victoire; Amor, Nawal; Fantin, Bruno; Wieder, Ingrid; Andremont, Antoine

DOI:
10.1101/196014
10.1038/s41564-018-0292-6

Document Version
Peer reviewed version

Citation for published version (Harvard):
Ruppé, E, Ghozlane, A, Tap, J, Pons, N, Alvarez, A-S, Maziers, N, Cuesta, T, Hernando-Amado, S, Clares, I, Martínez, JL, Coque, TM, Baquero, F, Lanza, VF, Máiz, L, Goulenok, T, de Lastours, V, Amor, N, Fantin, B, Wieder, I, Andremont, A, van Schaik, W, Rogers, M, Zhang, X, Willems, RJL, de Brevern, AG, Batto, J-M, Blottière, HM, Léonard, P, Léjard, V, Letur, A, Levenez, F, Weiszer, K, Haimet, F, Doré, J, Kennedy, SP & Ehrlich, SD 2019, 'Prediction of the intestinal resistome by a three-dimensional structure-based method', *Nature Microbiology*, vol. 4, no. 1, pp. 112-123. https://doi.org/10.1101/196014, https://doi.org/10.1038/s41564-018-0292-6

Prediction of the intestinal resistome by a 3D structure-based method

Etienne Ruppé* (1, 2), Amine Ghozlane* (1, 3, 4) Julien Tap*§ (1), Nicolas Pons (1), Anne-Sophie Alvarez (1), Nicolas Maziers (1), Trinidad Cuesta (5), Sara Hernando-Amado (5), Irene Clares (5), Jose Luís Martínez (5), Teresa M. Coque (6, 7, 8), Fernando Baquero (6, 7, 8), Val F. Lanza (6, 7), Luis Maiz (9), Tiphaine Goulenok (10), Victoire de Lastours (2, 10), Nawal Amor (10), Bruno Fantin (2, 10), Ingrid Wieder (11), Antoine Andremont (2, 11), Willem van Schaik (12, 13), Malbert Rogers (12), Xinglin Zhang (12), Rob J.L. Willems (12), Alexandre G. de Brevern (14), Jean-Michel Batto (1), Hervé M. Blottière (1), Pierre Léonard (1), Véronique Léjard (1), Aline Letur (1), Florence Levenez (1), Kevin Weiszer (1), Florence Haimet (1), Joël Doré (1), Sean P. Kennedy (1, 4), S. Dusko Ehrlich (1, 15)

(1) MGP MetaGénoPolis, INRA, Université Paris-Saclay, 78350 Jouy en Josas, France

(2) IAME, UMR 1137, INSERM, Paris Diderot University, Sorbonne Paris Cité,

(3) Bioinformatics and Biostatistics Hub, C3BI, Institut Pasteur, USR 3756 IP CNRS, Paris, France.

(4) Biomics, CITECH, Institut Pasteur, Paris, France.

(5) Centro Nacional de Biotecnología, CSIC, Madrid, Spain.

(6) Servicio de Microbiología. Instituto, Ramón y Cajal de Investigación Sanitaria (IRYCIS), Madrid, Spain

(7) CIBER en Epidemiología y Salud Pública (CIBER-ESP), Madrid, Spain

(8) Unidad de Resistencia a Antibióticos y Virulencia Bacteriana (RYC-CSIC), Madrid, Spain.

(9) Unit for Cystic Fibrosis, Ramon y Cajal University Hospital, Madrid, Spain

(10) Internal Medicine Department, Beaujon Hospital, AP-HP, Clichy, France

(11) Bacteriology Laboratory, Bichat-Claude Bernard Hospital, AP-HP, Paris, France

(12) Department of Medical Microbiology, University Medical Center Utrecht, Utrecht, the Netherlands

(13) Institute of Microbiology and Infection, University of Birmingham, Edgbaston, Birmingham B15 2TT, United Kingdom

(14) INSERM UMR_S 1134, Paris Diderot University, Sorbonne Paris Cité, Université de la Réunion, Université des Antilles, INTS, GR-Ex, Paris, France

(15) Centre of Host Microbiome Interactions, King's college, London, United Kingdom

*The authors equally contributed to the study

31

32 § Current affiliation: Danone Nutricia Research, Palaiseau – France

33

34 **Corresponding author**

35 Etienne RUPPE (PharmD, PhD)

36 Laboratoire de Bactériologie

37 Hôpital Bichat-Claude Bernard

38 46 rue Henri Huchard

39 75018 Paris

40 France

41 Phone: +33(0) 1 40 25 85 04

42 Fax: +33(0) 1 40 25 85 81

43 etienne.ruppe@inserm.fr

44

Opening paragraph

The intestinal microbiota is considered to be a major reservoir of antibiotic resistance determinants (ARDs) that could potentially be transferred to bacterial pathogens via mobile genetic elements (MGEs). Yet, this assumption is poorly supported by empirical evidence due to the distant homologies between known ARDs (mostly from culturable bacteria) and ARDs from the intestinal microbiota. Consequently, an accurate census of intestinal ARDs (*i.e.* the intestinal resistome) has not yet been fully determined. For this purpose, we developed and validated an annotation method (called pairwise comparative modelling, PCM) based on 3D structure (homology comparative modelling) leading to the prediction of 6,095 ARDs in a catalogue of 3.9 million proteins from the human intestinal microbiota. We found that the majority of predicted ARDs (pdARDs) were distantly related to known ARDs (mean amino acid identity 29.8%) and found evidence supporting their transfer between species. According to the composition of their resistome, we were able to cluster subjects from the MetaHIT cohort (n=663) into 6 “resistotypes” that were connected to the previously described enterotypes. Finally, we found that the relative abundance of pdARDs was positively associated with gene richness, but not when subjects were exposed to antibiotics. Altogether, our results indicate that the majority of intestinal microbiota ARDs can be considered as intrinsic to the dominant commensal microbiota and that these genes are rarely shared with bacterial pathogens.

Introduction

Antimicrobial resistance is one of the major threats to health identified by the World Health Organization for the next decades. The intestinal microbiota plays a pivotal role in this phenomenon as it harbours a vast diversity of bacterial species, some of them possessing antibiotic resistance determinants (ARDs) that may enable their survival under antibiotic exposure. Previous studies attempted to identify ARDs in the intestinal microbiota[2–4] but were confounded by the distant homologies between known ARDs (mostly from culturable bacteria) and ARDs from the intestinal microbiota (which are generally not cultured)[5,6]. For these reasons, bioinformatic tools based on sequence comparison (ARG-ANNOT[7], CARD – RGI[8], Resfinder[9], DeepARG[10]) or motif detection (Resfams[11]) are often unsuccessful in characterising the diversity of ARDs from metagenomic datasets. Indeed, there is no consensus on an optimal approach to detect ARDs in metagenomic datasets. Consequently, an accurate census of intestinal ARDs (*i.e.* the intestinal resistome) has not yet been fully determined.

While many bacteria have intrinsic, chromosomally-encoded ARDs and the capability of increasing resistance through mutation, they can also enrich their resistance capabilities through the acquisition of exogenous ARDs located on mobile genetic elements (MGEs) such as plasmids, transposons or phages. The intestinal microbiota harbours thousands of bacterial species including well-known pathogens (e.g. *Enterobacteriaceae* and *Enterococcus spp*.). This unique environment is assumed to be a reservoir of ARDs that can potentially be transferred to bacterial pathogens[13]. Nonetheless despite the high selective pressure exerted on the intestinal microbiota by over seven decades of intensive antibiotic usage, a very low number of transfer events from an intestinal commensal to a bacterial pathogen have been observed[14,15]. This challenges the hypothesis of a mobile resistome and the assumption that the intestinal microbiota serves as a reservoir of ARDs to which pathogenic bacteria have easy access[16]. In this study, our objective was to perform an extensive characterization of the human gut resistome (including the capacity of ARDs to transfer between species) and to assess its dynamics under various antibiotic exposures.

Prediction of ARDs in the intestinal microbiota

To predict ARDs in the intestinal microbiota, we developed a method based on protein homology modelling (see methods) that we termed PCM (for “pairwise comparative modelling”). PCM is a generic method using homology modelling to increase the specificity of functional prediction of proteins,

especially when they are distantly related to potential homologs. PCM uses a list of reference proteins sequences from a given family, the ARD structures of this family (used as structural templates in protein data bank [PDB] format) and a series of negative references (Figure 1A, Supplementary Figure 1, 2 and 3). Structural models are built using both the ARD reference and negative reference templates. Scores generated from both positive and negative references are used to determine which model performed the best. This is done using a machine-learning algorithm trained on 662 ARD and 522 negative references. The PCM score equals the number of times the query was classified as an ARD for the bootstraps performed, expressed as a percentage. Candidates with a PCM score ≥50% and an alignment score with the reference template (TM score given by TM-align) ≥0.5[17] were predicted as ARDs.

The performance of PCM to predict ARDs was assessed using *in vitro* and *in silico* methods. We synthesized 71 candidate ARDs from 12 families (Table 1), and expressed them in *Escherichia coli* (see methods). All 12 pdARDs sharing an amino acid identity >95% with a known ARDs had a detectable resistance activity against antibiotics (Figure 1B). Resistance activity was also detected in 35/41 (85.3%) of the predictions made with a good level of confidence (PCM score >99%, Tm score TmAlign>0.9) and in 8/18 (44.4%) of the predictions with a lower level of confidence (PCM score <80%, Tm score TmAlign<0.8). The mean amino acid identity of the functional pdARDs (good and fair predictions, n=43) with known ARDs was 28.6% (range 19.4%-82.6%, Supplementary Table 1). We then tested PCM against an experimentally-validated functional metagenomics dataset from soils[18]. In this case, PCM was able to accurately identify 1,374 ARDs out of 1,423 hits (sensitivity 96.6%) (see methods). Finally, we assessed the performances of PCM with incomplete proteins as inputs, and showed that PCM could correctly predict ARDs when the available amino acid sequence was at least 40% complete (Supplementary Figure 4). After the *in vitro* and *in silico* validation of the method, we used PCM to search for ARDs in the in a catalogue made of 3,871,657 proteins which was built from the sequencing of faecal samples of 396 human individuals (177 Danes and 219 Spanish) recruited in the MetaHIT project[19]. In total, we predicted 6,095 ARDs (0.2% of the catalogue) from 20 ARD classes conferring resistance to nine major antibiotic families[20]: beta-lactams (class A, B1-B2, B3, C and D beta-lactamases), aminoglycosides (AAC(2'), AAC(3)-I, AAC(3)-II, AAC(6'), ANT, APH, RNA methylases), tetracyclines (Tet(M), Tet(X)), quinolones (Qnr), sulphonamides (Sul), trimethoprim (DfrA), fosfomycin (Fos) and glycopeptides (Van ligases) (Table 1 and Supplementary Table 1). With the same, extensively curated

reference ARDs census as input, only 67 ARDs would have been predicted according to conventional BLASTP[21] search with a specific identity threshold (80% over 80% of the reference sequence)[3,4]. ARG-ANNOT[7], Resfinder[9] and DeepARG[10] were able to predict 54, 50 and 2,139 ARDs, respectively, while Resfams[11] predicted a very high number of ARDs (44,105). The HMM-based search for class B1 beta-lactamases published by Berglund *et al*.[22] also yielded a high number of hits (n=3,490) in the 3.9 million protein catalogue (Figure 1C, Supplementary Figure 5). Further analysis on a catalogue of dummy, synthetic 3.9 million proteins indeed showed that Resfams, DeepARG and the Berglund *et al*. HMM-based search lacked specificity (see Supplementary Information). The mean identity shared between predicted (n=6,095) and reference ARDs was 29.8%; it was significantly higher than candidates not predicted as ARDs (mean 23.0%, Wilcoxon unpaired test p=2e-16, Figure 1D). Indeed, most of the pdARDs were distantly related to reference ARDs (Supplementary Figure 6 and 7). Besides, PCM failed to predict 16 ARDs which shared at least 40% identity with a reference ARD (Supplementary Table 2). The 6,095 pdARDs and their structures are available at http://mgps.eu/Mustard.

Taxonomic distribution of ARDs

A host bacterial phylum could be assigned to 72.3% (4405/6095) pdARDs. The majority was identified as from the dominant human intestinal phyla Firmicutes (2962/4405, 72.3%) and Bacteroidetes (858/4405, 19.5%) (Supplementary Figure 8) with only 5.8% (225/4405) of pdARDs coming from Proteobacteria. An additional seven pdARDs were predicted to be harboured by Archaea (*Methanobrevibacter* and *Methanoculleus* genera), putatively conferring resistance to macrolides, tetracyclines, aminoglycosides, sulphonamides and glycopeptides (Supplementary Table 1). We also predicted ARDs in genera of medical interest where no ARDs had been identified such as *Akkermansia*[23] (10 pdARDs) and *Faecalibacterium*[24] (44 pdARDs). Only 23 out of 6,095 (0.4%) had been previously identified in families and genera that include human pathogens (Enterobacteriaceae, *Campylobacter*, *Enterococcus*, *Streptococcus* and *Acinetobacter*). The distribution of the families of pdARDs differed according to the phyla (Supplementary Figure 9): Firmicutes and Proteobacteria were enriched with aminoglycosides-modifying enzymes (AMEs, spanning APH, ANT, and AACs) whereas Bacteroidetes were enriched in Sul and class A beta-lactamases. Interestingly, the tigecycline-degrading monooxygenase Tet(X) was frequently found in Bacteroidetes and Proteobacteria, the two phyla between which transfer of the *tet(X)* gene has been reported[14,25]. In order to support these assignments,

we sequenced the metagenome of four human faecal samples before and after an overnight culturing using conditions that favoured the growth of oxygen-tolerant bacteria such as Enterobacteriaceae and enterococci (see methods). The results showed an enrichment of Proteobacteria (over Firmicutes and Bacteroidetes), and a commensurate increase of class C beta-lactamases, Fos and Tet(X), along with Van ligases (Supplementary Figure 10).

Location of the pdARDs and association with mobile genetic elements

We investigated the potential for mobility of the pdARDs at different levels. First, we took advantage of the identification of gene clusters based on co-abundance and co-occurrences of genes among the 396 faecal metagenomes used to build the 3.9 million MetaHIT gene catalogue[19]. A total of 7,381 gene clusters referred to as metagenomic units (MGUs) were identified. Among MGUs, metagenomic species (MGS) are defined as MGUs with ≥700 genes, which are considered to be representative of partial or complete bacterial genomes[19]. MGUs of <700 genes include MGEs such as plasmids, phages, transposable elements, and incomplete chromosomal sequences. The 7,381 MGUs from the 3.9 million gene catalogue of intestinal microbiota gene were queried with the pdARDs. A total of 3,651 (59.9%) pdARDs could be mapped onto an MGU. The distribution of pdARDs as a function of MGU size is shown in Figure 2A. Most (95.6%, 3,489/3,651) pdARDs mapped onto MGS and the relative abundance of pdARDs correlated strongly with the abundance of their respective MGS (Supplementary Information), supporting their location on the same bacterial host across the 396 individuals. We also searched for pdARDs in metagenomic species pan-genomes (MSPs)[26] obtained from the 9.9 million intestinal gene catalogue[27]. Similar to MGS, MSPs are clusters of genes that are co-abundant in a set of sample. In MSPs, genes that are constantly found are referred as “core” while inconsistently found genes are referred to as “accessory”. Besides, “shared core” genes are assumed to be conserved genes shared between phylogroups[26]. We found 4,912 pdARDs located on MSPs, with the majority being assigned to the core pangenome (4,099/4,912, 83.4%) or shared between core-pangenomes (389/4,912, 7.9%). This was different with MGE-associated genes[27] with most being not found in MSPs (Figure 2B).

Then, we investigated whether genes associated with gene mobility (transposases, conjugative elements and integrons) were present on the same contig than the pdARDs. We found that 7.9% (484/6,095) of pdARDs were co-located with homologs of MGE-associated genes. For pdARDs not

found in MGS or in MSPs (n=974), 876 (89.9%) had no detectable MGE-associated genes in their vicinity.

Finally, we searched for pdARDs homologs (BLASTN >97% identity over >90% of the query length) in the Genbank database (2018 July 11). Only 538 pdARDs homologs were identified, with 49 being located on a plasmid and/or a phage (Supplementary Table 3). Among the 489 remaining pdARDs, 82 (16.8%) were found in multiple species, mainly (60/82, 73.2%) from the same genus (Supplementary Table 4).

The phyla Bacteroidetes, Firmicutes and Tenericutes had the higher proportions of ARDs co-locating with MGEs (Figure 2C). No ARD family was found to be enriched in MGE, with the exception of the Tet(X) family in which 3 out of 9 (33.3%) predictions (2 from *Bacteroides fragilis* and 1 from *E. coli*) were associated with transposases (Figure 2D).

Distribution of pdARDs in human hosts' microbiota

In the MetaHIT cohort (663 subjects), we found that subjects carried pdARDs with a median relative abundance of 0.22% (range 0.14%-0.38%), with pdARDs from the Tet(M) family being the most abundant (0.07%) and those from class B3 beta-lactamases the least (median: 0.004%). The average number of unique pdARDs genes detected per metagenome was 1,377 (range 258-2,367). Most pdARDs were shared across multiple subjects, 987/6,095 (16.2%) were found in at least 50% of individuals, and only 106/6,095 (1.7%) occurred uniquely in a single individual. All ARD families, with the exception of RNA methylases and AAC(2') families, were found in more than 80% of individuals.

Then, we assessed whether subjects with no recent exposure to antibiotics could cluster according to their intestinal resistome. Based on the pdARDs family patterns, six clusters (that we named "resistotypes" by analogy with the enterotypes[28]) were detected using Dirichlet multinomial mixture models (Supplementary Figure 11). The four most frequent resistotypes each represented around 20% of the cohort (the fifth and the sixth representing 8.7% and 7.5%, respectively). The three first resistotypes were characterized by a high abundance of Van ligases (Supplementary Figure 12). Resistotype 1 was enriched in ANT, while resistotype 3 was driven by Tet(M) and class C beta-lactamases. Resistotype 4 was enriched with Tet(X) and class A beta-lactamases and resistotype 6 in class B1 beta-lactamases and Sul. We observed that resistotypes, as determined by PCM, were highly connected to the composition of the microbiota, and that this effect was more pronounced than

resistotypes determined from the results of BLASTP and Resfams (Figure 3A). The resistotypes of the MetaHIT cohort were found to be associated with enterotypes (chi square test, p=5e-4), Figure 3B-D, Supplementary Figure 13). Resistotypes 1 and 3 had higher gene richness and were associated with the Clostridiales–driven enterotype. Resistotype 4 was more prevalent in enterotypes driven by Bacteroides (known to harbour Tet(X) and class A beta-lactamases) while resistotype 6 was very specific to the *Prevotella* enterotype (Figure 3C-D). The relative abundance of pdARDs was observed to be positively correlated to the gene richness (Figure 4A, Spearman's rank correlation test Rho=0.31, p=5e-16). Conversely, we did not find any link between resistotypes and body mass index, age or gender.

Dynamics of the pdARDs under various exposures to antibiotics

We investigated the abundances of pdARDs in subjects under various exposures to antibiotics and healthcare environments. Three types of exposure were considered (see methods for details): hospitalization in a French hospital without receiving antibiotics, n=15, chronic exposure (Spanish cystic fibrosis patients frequently exposed to antibiotics, n=30) and short high-dose exposure through selective digestive decontamination [SDD; oral colistin, tobramycin, antifungal amphotericin and parenteral cefotaxime[29]] at admission in intensive care units in Netherlands, n=10). We again confirmed a positive correlation between relative abundance of pdARDs and gene richness among patients unexposed to antibiotics (Figure 4B, Spearman's rank correlation test Rho=0.37, p=0.01, see methods). However, when all the samples were considered, including those with antibiotic exposure, this relationship was no longer present (Figure 4C). Instead, the relative abundance of pdARDs was found to be higher in subjects with a chronic exposure than in subjects with no recent exposure (Figure 4D, Wilcoxon unpaired test, p=1e-10), and gene richness was lower (Figure 4E, Wilcoxon unpaired test, p=0.006) In particular, subjects with chronic exposure carried more class B1-B2 beta-lactamases, AAC(6'), ANT, APH, Erm, and DfrA with lower abundance of Sul (Supplementary Figure 14). At the phylum level, we observed a decrease of Bacteroidetes and Verrucomicrobia and an increase of Firmicutes and Actinobacteria in patients chronically exposed to antibiotics (Supplementary Figure 15). A total of 74 MGS were found to be differentially abundant among subjects with or without chronic exposure to antibiotics (Supplementary Table 5).

This was different with subjects before and after SDD. A drastic loss of gene richness was measured for this group (Figure 4E): from a mean of 295,919 genes to 95,286 (67.8 % reduction, Wilcoxon paired test, p=0.006). Meanwhile, the relative abundance of pdARDs did not change significantly (Figure 4D, p=0.4). At the ARD family level, we observed that some families decreased significantly: class C beta-lactamases (commonly found in Enterobacteriaceae and Pseudomonadaceae which are specifically targeted by SDD), Fos, Tet(X), APH and ANT (Supplementary Figure 16). We then analysed the MGS at the phylum level and found that Proteobacteria, Actinobacteria, Firmicutes and Fusobacteria decreased significantly after SDD (Supplementary Figure 17). A total of 358 MGS were found in this cohort and, despite the small number of subjects (n=10), we found 133 MGS for which a significant variation was observed (Supplementary Table 6). We tested whether a high abundance of pdARDs could be protective against the antibiotics used in SDD, but found no association: the relative abundance of pdARDs before SDD was not linked to the gene richness after SDD. Hospitalization without antibiotic therapy, that is, potential exposure to antibiotic-resistant nosocomial pathogens without selective pressure, did not affect the gene richness nor the relative abundance of pdARDs (Figure 4D and 4E).

Discussion

The results of this study support the concept that the majority of ARDs from the intestinal microbiota are hosted by commensal bacteria, and that their transfer between species (including to opportunistic pathogen) is rare[30]. We provide several findings to support this assumption: 1) we used a 3D structure-based method to assess the diversity of ARDs in the intestinal microbiota and confirmed that ARDs predicted by PCM in the intestinal microbiota were distantly related to known ARDs, 2) the sensitivity and the specificity of the method was validated by gene synthesis of a subset of predictions and by benchmarking against various datasets (functional metagenomic of the soil microbiota, genomes and random protein catalogues), 3) the majority of pdARDs could be found in clusters of co-abundant genes (MGS and MSPs) in large cohorts of samples, while only a minority was found on plasmids, phages or in the vicinity of MGE-associated genes, 4) we could stratify subjects into 'resistotypes' that were connected to enterotypes, and 5) gene richness, otherwise associated with a healthy status[31], was positively correlated to the abundance of ARDs in subjects not exposed to antibiotics.

Our results challenge the paradigm that ARDs of the intestinal microbiota are a threat to public health. As was previously demonstrated for environmental samples[18,32], ARDs tend to cluster according to the

underlying microbial ecology of the ecosystem, suggesting that the vast majority of ARDs are fixed in their microbial hosts and are not, or very rarely, transferred. Our results show that the dominant intestinal microbiota are not a major conduit through which opportunistic pathogens can acquire ARDs. Nevertheless, we acknowledge that such transfer events have been reported[14,15] and that consequences for public health can be important, as in the case of the *vanB* vancomycin resistance operon that is shared by *Clostridium* spp. and enterococci[15]. Understanding the mechanisms that can lead to the mobilisation of ARDs in the intestinal microbiota, as well as a broader census of environmental reservoirs of ARDs (e.g. sewage, livestock, the subdominant human intestinal microbiota) will continue to be an important area for future research.

We found that subjects cluster according to the composition of their resistome into six groups that we named “resistotypes” (as a reference to the previously described enterotypes[28]). These resistotypes were indeed connected to the enterotypes. Description of this underlying structure is interesting as one might hypothesize that a particular resistotype, or microbiota enriched with ARDs, might be affected to different degrees by antibiotic therapy. This has previously been observed for beta-lactamase-producing *Bacteroides* which can protect the microbiome against exposure to β-lactams[33]. In patients undergoing faecal microbiota transplantation, follow-up antibiotic therapy may be adjusted to favour engraftment of the donor microbiota[34]. Identifying donors with a resilient microbiota, due to a protective resistotype, could open perspectives for the optimisation of the clinical implementation of faecal microbiota transplants.

Contrary to initial expectations, some pdARD families decreased in their abundance under antibiotic exposure, especially when patients were exposed to a combination of antibiotics (such as SDD). In order to resist to a combination of antibiotics, bacteria would need to be intrinsically resistant or to acquire an adequate combination of ARDs. The dynamics of ARDs under antibiotic exposure depend on various parameters: spectrum of the ARD (the level of resistance towards the antibiotic provided by the ARD), the expression level of the ARD, and the presence of other resistance mechanisms (intrinsic or acquired). The large number of possible combinations of these factors can explain that in some situations, a bacterium can be inhibited by antibiotics despite the presence of a putatively compatible ARD. Alternatively, we cannot exclude that changes in pdARDs families could also be explained by simple taxonomic shifts that are not connected to the antibiotics studied.

The limitations of current techniques and of this study leave a number of important questions unresolved. As mentioned earlier, metagenomic sequencing provides information for the dominant fraction of intestinal bacteria, and so ARDs present in subdominant bacteria remain unobserved. Indeed, several ARDs found in opportunistic pathogens among the Enterobacteriaceae (e.g. *Escherichia coli* and *Klebsiella pneumoniae*) originate from other species in the same Proteobacteria phylum[35]. A recent study indeed cultured many Proteobacteria species that were not detected in metagenomic sequencing[36]. We cannot rule out that the subdominant bacteria, which were not probed by metagenomic sequencing, could be an additional reservoir of ARDs. In terms of the clinical samples analysed, we cannot exclude that the differences between patients and controls may be resulting from confounding factors other than the antibiotic exposure.

The method we used to identify distantly related proteins is based on homology modelling and takes advantage of the observation that proteins sharing the same function have more similar structures than amino acid sequences[37]. Indeed, PCM could identify functional ARDs with amino acid identity below 20% to known ARDs. Notably, PCM can only be used to predict the function of genes that are homologous to known ARDs, and therefore the identification of different classes of ARDs with no homology to known ARDs will still require functional screening. Besides, while PCM was validated in this study, it remains a prediction tool. While similar structures are usually indicative of similar function, this is not always the case and PCM can yield false positives results (as observed in the functional validation of synthesized pdARDs). Due to the scope of our study, gene synthesis validation was not performed for all ARD families, leaving open the possibility that not all pdARDs identified here truly have a role in antibiotic resistance.

In summary, we developed a method, PCM, which could unveil the diversity of ARDs in the intestinal microbiota. Employing this tool, we gathered evidence that the vast majority of the ARDs we predicted showed no sign of mobility and that their abundance was correlated to gene richness. Together with the protective trait of some intestinal bacteria against antibiotics[33], our results suggest that the ARDs from the intestinal microbiota might be considered as our “resilience allies”[38] assuring the preservation of the healthy commensal microbiota under antibiotic exposure.

Acknowledgements

The authors are deeply grateful to the GENOTOUL (Toulouse, France), GENOUEST (Rennes, France), ABIMS (Roscoff, France), MIGALE (Jouy-en-Josas) and TGCC-GENCI (Institut Curie) calculation clusters. The authors also warmly thank Bruno Perichon (Institut Pasteur, Paris, France) for providing ARD sequences from *Acinetobacter baumannii,* Patricia Siguier (CNRS, Toulouse, France) for helping the search of insertion sequences with ISfinder, Julien Guglielmini (Institut Pasteur, Paris, France) for his assistance in finding conjugative elements, Stevenn Volant (Institut Pasteur, Paris, France) for the design of the statistical model in SHAMAN, Thomas Jové (University of Limoges, France) for his assistance in finding integrons, Marie Petitjean (IAME Reserch Center, Paris, France) for her assistance in bioinformatic analyses, Florian Plaza-Oñate and Mathieu Almeida for their help with MSPs.

Funding

The project was funded in part by the European Union Seventh Framework Programme (FP7-HEALTH-2011-single-stage) under grant agreement n° 282004, EvoTAR. IRYCIS authors acknowledge the European Development Regional Fund “A way to achieve Europe” (ERDF) for co-founding the Spanish R&D National Plan 2012-2019 Work (PI15-0512), CIBER (CIBERESP; CB06/02/0053), and the Government of Madrid (InGeMICS- B2017/BMD-3691). Val F. Lanza was further funded by a Research Award Grant 2016 of the European Society for Clinical Microbiology and Infectious Diseases (ESCMID).

Conflicts of interest

None.

Authors’ contribution

ER, AG, JT performed the analysis. ER, AG, JT, WvS, AdB and SPK wrote the manuscript. ASA and NM handled the data management. TC, SHA, IC and JLM performed the gene synthesis experiments. JLM, TMC, VFL, FB, AdB, JD, SPK, FH and SDE discussed the protocol and results. LM, TG, VdL, NA, BF, IW, AA, WvS, MR, XZ and RJL recruited the patients and collected the samples. HB, VL, AL and FL handled the wet lab experiments. NP, PL and JMB managed the informatics and the calculation clusters. KW and NP designed the website (http://mgps.eu/Mustard/).

Methods

Constitution of the databases of antibiotic resistance determinants

We define as an ARD as in Martinez *et al*[39]: a protein encoded by a gene that confers resistance to antibiotics when it is present or increases susceptibility to antibiotics when it is absent. This definition excluded housekeeping genes in which mutations can confer resistance to some antibiotics (such as topoisomerases in which mutations can lead to fluoroquinolone resistance) and genes involved in the regulation of antibiotic resistance genes. Also, we excluded efflux pumps such as TetA or QepA as very few or no PDB are available, presumably due to the difficulty to crystallize transmembrane proteins. Amino acid sequences of functionally characterized ARDs from the major antibiotic families used in human medicine (beta-lactams, aminoglycosides, tetracyclines, trimethoprim, sulfonamides, macrolides-lincosamides-synergistines, fluoroquinolones, fosfomycin and glycopeptides)[20,40] were obtained from the following antibiotic resistance databases: Resfinder[9], ARG-ANNOT[7], the Lahey Clinic (http://www.lahey.org/studies/), RED-DB (http://www.fibim.unisi.it/REDDB/), Marilyn Roberts's website for macrolides and tetracycline resistance genes (http://faculty.washington.edu/marilynr/) and from functional metagenomics studies[5,6,41]. When ARDs were provided as nucleic acids sequences, they were translated into proteins with Prodigal[42]. Non-redundancy of the reference ARDs was assessed with CD-HIT v4.5.7[43] (100% identity). The final database was manually curated in order to remove incomplete sequences and ARDs from families not considered in this work. The cluster of orthologous genes (COG) of each member of the reference dataset was assigned from the v3 eggNOG database[44]. In total, we collected 1,651 non-redundant amino acid sequences spanning 20 ARDs families: Class A beta-lactamases (Blaa), class B1-B2 beta-lactamases (Blab1), class B3 beta-lactamases (Blab3), class C beta-lactamases (Blac), class D beta-lactamases (Blad), aminoglycoside acetyltransferases (AAC) AAC(2'), AAC(3)-I, AAC(3)-II, and AAC(6'), aminoglycoside nucleotidyltransferases (ANT), aminoglycoside phosphotransferases (APH), 16S rRNA methylases, Tet(M), Tet(X), type A dihydrofolate reductases (DfrA), dihydropteroate synthases (Sul), erythromycin ribosome methylases (Erm), quinolone resistance proteins (Qnr), fosfomycin resistance proteins (Fos), and D-Ala – D-Lac/Ser ligases (Van) (Table 1). The recently described plasmid-mediated colistin resistance *mcr-1* gene[45] could not be included because of the lack of a reliable PDB template obtained by X-ray diffraction at the time of the study.

Interrogation of the catalogue for ARDs

We used a 3,871,657 million proteins catalogue previously published[19]. This catalogue was built from the metagenomic sequencing of the faeces of 396 subjects from Denmark and Spain. In brief, the 3.9 million gene catalogue results from a non-redundancy filtering at 95% nucleic acid identity and 90% coverage: predicted genes from all samples (45.4 million in total) were clustered using BLAT by single linkage. Any two genes with greater than 95% identity and covering more than 90% of the shorter gene were clustered together. The contigs were originally built using SOAPdenovo (from the MOCAT pipeline[52]). We selected this catalogue over the more recent 10 million gene catalogue that was published during the course of this study[27] because metagenomic units (MGUs, including the metagenomic species [MGS]) had been determined only for the 3.9 million gene catalogue. The genes of the catalogue were translated into proteins using Prodigal[42] using the –p meta option. For each ARD family, we searched for ARDs using the three following methods: (*i*) we built a hidden Markov model file for each ARD family and searched the catalogue with Hmmsearch (v3. 1)[46], (*ii*) we performed a Smith-Waterman alignment with a heuristic seed detection (BLASTP v. 2. 2. 28+)[21] and (*iii*) a rigorous Smith-Waterman search (SSearch v. 36. 3. 6)[47] with an E-value threshold of 1E-5. Only the hits with a size ranging from 75% and 125% of the mean amino acid size of the ARD family were further considered. All candidates were assigned a COG/NOG from eggNOG v3[44]. When candidates were found in different ARD families (e.g. a candidate could be a hit in class B1-B2 and class B3 beta-lactamases), the candidate was assigned to the family for which it had the highest amino acid identity with the reference.

Negative references

For each ARD family, COGs/NOGs were attributed to reference ARDs. In parallel, the COGs/NOGs were attributed to the hits obtained during the initial steps of PCM (i.e. the hits obtained by the BLASTP/SSearch and Hmmer search). In the list of candidates from a given ARD family, the COGs/NOGs that were not found in the COGs/NOGs attributed to reference ARDs were assumed to be potential COGs/NOGs from false positives hits (Supplementary Figure 2) as it reproduced the errors of functional assignment likely to be generated in sequence-only annotations. The amino acid sequences of the representative proteins from those COGs/NOG groups were obtained from the eggNOG v3 database, and were added to the negative reference dataset. A manual curation step was performed in order to ensure that no references were included in the negative references.

Selection of structural templates

The list of protein structures that could be used as structural templates was downloaded (June 2014, and November 2014) from the PDB library (Protein DataBank[48], http://www.rcsb.org/). Using the reference dataset and the negative references described above, Hmmer[46], BLASTP[21] and SSearch[47] were performed on the PDB database with default settings and E-values of 1E-5. Results were merged into a non-redundant PDB list. Both lists (references and negative templates) were manually curated to ensure that no references were represented in the negative templates dataset, and vice versa. If more than one PDB shared the same UniProt number (i.e. if the structure of a protein has been determined on multiple occasions), we filtered the PDB files in order in include a unique structure per UniProt number using the following positive criteria: absence of ligand, completeness of the protein and high resolution.

Pairwise comparative modelling

The concept of pairwise comparative modelling (PCM) is shown in Supplementary Figure 1-3 and the framework is available at https://github.com/aghozlane/pcm. The concept of leveraging the protein structure in complement to its amino acid sequence was motivated by the fact that proteins sharing common functions would be more conserved in the active site which cannot be observed by the analysis of protein sequence alignments [37]. Each candidate was subjected to homology modelling with reference templates and negative templates, generating two 3D structures for each candidate (Fig 1A). The main idea is that if a sequence is truly functionally related to the reference fold, its model must be significantly different from the ones obtained with the negative structural template. Homology modelling was performed by PCM in six main steps (example in Supplementary Figure 3):

1. Three structural templates were identified by BLASTP (among the lists produced as described above) that shared the highest amino acid identity with the candidate protein.
2. A multiple sequence alignment was performed between the candidate and the three templates sequences using Clustalo[49].
3. A prediction of the secondary structure was performed using psipred (v3.5)[50]. The residues predicted to fold in helix or in beta-sheet conformation with a level of confidence higher or equal to 7 were considered to constrain the model.

4. A comparative modelling was performed with the MODELLER programming interface[51]. MODELLER automatically calculates a model by satisfaction of spatial restraints such as atomic distance and dihedral angles in the target sequence, extracted from its alignment with the template structures. Stereo-chemical restraints for residues are obtained from the CHARMM-22 molecular force field and statistical preferences obtained from a representative set of known protein structures.

5. The best model out of a hundred produced by MODELLER (based on the Dope score) was considered for structure assessment analysis using ProQ[52] and Prosa-web[53]. The Dope score (Modeller), z-score (Prosa), MaxSub and LG score (ProQ) are statistical potential variables used to predict the model quality. Both ProQ and Prosa-web are trained on the PDB to determine real protein configuration and they estimate the energetic favourability of the conformation of each residue in the model.

6. The best model was aligned with the reference set of structures using TM-align[17] and MAMMOTH[54]. The RMSD (TM-align), z-score (MAMMOTH), TM-score (MAMMOTH, TM-align) estimates the degree of superposition of the residue between two structures.

The differences (delta) between the scores determined from each modelling path (with the reference set or the negative set) were calculated and used for the PCM machine learning program (see below).

For one given candidate, the PCM whole process took an average of 8 CPU-hours (30 minutes on 16 CPUs).

Taxonomic assignation

pdARDs were taxonomically assigned by combining the results obtained from BLASTN against the NCBI Genomes database (minimal 70% identity and 80% coverage), a BLASTN against the IMOMI in-house database (minimal 85% identity and 90% coverage) and the taxonomy of the metagenomic unit whenever applicable. The lowest taxonomic rank from the results of the three methods was assigned to the pdARD.

Statistical analysis

To discriminate reference proteins from negative references, we used model quality predictors and alignment scores (inferred from the semi-automatic pipeline described above) and developed a custom pipeline in R (R Core Team, 2013, http://www.R-project.org) to perform the classification. The LASSO

penalized logistic regression[55] implemented in LIBLINEAR[56] was used to compute the classifier. Ten-fold stratified cross validation (re-sampled 100 times to obtain more stable accuracy estimates) was used to partition the data into a training and test sets. The LASSO hyper-parameter was optimized for each model in a nested 5-fold cross-validation on the training dataset using the area under curve (AUC) as the model selection criterion. From the 100 times re-sampled ten-fold cross validation, receiver operating characteristic (ROC) analysis was used to evaluate model performance using the median AUC. Coefficients extracted for each modelling or alignment score were also evaluated for their stability throughout the computed models. The PCM score was the ratio (expressed as a percentage) between the numbers of time a candidate was classified as a reference and the number of bootstraps. Predicted ARDs were candidates with a PCM score ≥50% and a TM score given by TM-align ≥0.5[17]. To control how structural modelling brought additional information compared to amino acid sequence alignment only, we built a logistic regression model based on T-coffee alignment score (R glm, ten-fold stratification, re-sampled 100 times). We then compared the two classifiers models used for PCM and for T-coffee alignment based on the reference set (see Supplementary Information).

Validation of the method with a functional metagenomic dataset

The performance of PCM was assessed by analysing the data in Forsberg *et al*., where the ARD content of different North American soils was analysed using functional metagenomics[18]. The screening of the clones was performed on aztreonam, chloramphenicol, ciprofloxacin, colistin, cefepime, cefotaxime, cefoxitin, D-cycloserine, ceftazidime, gentamicin, meropenem, penicillin, piperacillin, piperacillin-tazobactam, tetracycline, tigecycline, trimethoprim and trimethoprim-sulfamethoxazole (cotrimoxazole). Here, we collected the nucleotide sequences of the inserts deposited on Genbank (KJ691878–KJ696532). The sequence translation of the open reading frames was performed by Prodigal (using default parameters)[42]. A total of 4,654 insert sequences were collected, in which 12,904 amino acid sequences were predicted. We then searched for ARDs belonging to the relevant ARD families according to the antibiotics used for the screening of the clones: beta-lactamases (all classes), APH, ANT, AAC(2'), AAC(3)-I, AAC(3)-II, AAC(6'), RNA methylases, Tet(M), Tet(X), Qnr, Sul and DfrA, using the Supplementary Table 2 of the Forsberg *et al.* paper. Inserts with no putative ARDs (according to the annotation of the gene) were removed (n=269). Inserts selected on cycloserine (n=868) and chloramphenicol (n=129) were not considered here because they were not included in the 20 ARD

families in this work. Fourteen inserts which contained more than one putative ARD that could be identified to confer resistance to the antibiotic used for the screening (e. g.; two beta-lactamases) were not considered in this analysis. An additional 1,658 inserts containing no putative ARDs or a putative ARDs that did not confer resistance to the antibiotic used for selection were discarded and so were 294 inserts containing efflux pumps, as these were not considered in this study. The resulting validation set contained 1,423 inserts (with resistance genes) for a total of 3,778 genes. To compare the outcome of PCM with other tools, the results for class B1-B2 and B3 beta-lactamases generated by PCM were merged into one class B beta-lactamases group as other tools do not separately consider the different class B beta-lactamases.

In total, 1,390 unique hits were found during the initial screen of PCM, of which 1,374 were predicted as ARDs (Supplementary Table 7). Among the 33 ARDs not included for PCM, 12 were not considered because they were undersized and 10 because they were oversized. No hits for AAC(2'), ANT, Qnr or Sul were found. The mean identity shared with reference ARDs was 37.6% (range 18.8-94.5). Overall, the sensitivity was 96.6%, with no false negative. In comparison, only 8 ARDs would have been identified by a conventional method (combination of Hmmsearch, BLASTP and SSearch with both a minimal identity with a reference ARD and coverage over or equal to 80%). Conversely, Resfams[11] that was specifically designed to identify ARDs from functional metagenomic datasets showed a similar sensitivity to PCM with the identification of 1,346 ARDs out of 1,423 (94.6% sensitivity).

Validation of the method for incomplete genes

The 3.9 million gene catalogue harbours 41.4% of genes that are predicted to be incomplete either on the 5', the 3' or both extremities[19]. As the size parameter is crucial for homology modelling, we tested to what extent the prediction of incomplete ARDs by PCM could remain valid. We selected 12 reference class A beta-lactamases (BlaZ, CblA-1, CepA-29, CfxA2, CfxA6, CTX-M-8, KPC-10, OXY-1, PER-1, SHV-100, TEM-101 and VEB-1) and we then iteratively removed 5% of the amino acid sequence at both edges in order to obtain 16 bi-directionally trimmed candidates (from 100% to 25%) per reference ARD. Candidate genes were chosen to span the diversity of known beta-lactamases, but the main representative beta-lactamase of the subfamily (e.g. TEM-1 for TEM beta-lactamase) was not necessarily chosen. Note that SHV-100 has a slightly longer sequence (13 amino acid duplication) than other SHV. A total of 192 PCM experiments were performed: we observed that the 12 references were

correctly predicted as ARDs when at least 40% of the protein remained (i.e. 30% trim from each extremity, Supplementary Figure 4). Thus, we are confident that with the 75% size threshold used in this study (a maximum of 25% removed from one edge), no misclassification due to an incomplete gene would be expected.

Gene synthesis

We selected 71 pdARDs from 12 ARD families: 14 from class A beta-lactamases, 8 from class B1-B2 beta-lactamases, 7 from class B3 beta-lactamases, 4 from class C beta-lactamases, 2 from class D beta-lactamases, 2 AAC(3)-I, 5 AAC(3)-II, 8 AAC(6'), 3 ANT, 4 APH, 13 Tet(M) and 1 Tet(X)) for gene synthesis and sub-cloning into *Escherichia coli* to test the decrease of susceptibility to antibiotics. For beta-lactamases, a chromogenic test (nitrocefin) was used to detect function. Minimal inhibitory concentrations (MIC) were determined by E-Test strips (bioMérieux, Marcy-l'Etoile, France) in duplicate. A pdARD was considered to have an activity against an antibiotic (tobramycin for AAC(3)-I, AAC(3)-II, AAC(6') and ANT; kanamycin for APH and tetracycline for Tet(M)) when the MIC of the clone was above the MIC of a clone harbouring the plasmid without a synthesized gene or when the colour of the broth containing nitrocefin turned red, in the case of beta-lactamases. We used the plasmid vector pET-22b+ (embedding a beta-lactamase – encoding gene) for pdARDs hypothesized to confer resistance to aminoglycosides and the pET-26b (embedding a gene conferring resistance to kanamycin) for the other pdARDs. The selection of the pdARDs for synthesis was performed as follows:

- References (n=12): pdARDs which shared a high identity with known ARDs (≥95% amino acid identity and ≥80% coverage with a reference ARD).
- Good predictions (n=41): pdARDs with the highest degree of confidence for the prediction (PCM score >99%, Tm score TmAlign>0.9 and <70% amino acid identity with a reference ARD.
- Fair predictions (n=18): pdARDs with the lowest degree of confidence for the prediction (PCM score <80%, Tm score TmAlign<0.8 and <70% amino acid identity with a reference ARD).

Signatures of mobile genetic elements nearby the predictions of ARDs

We searched for mobile genetic elements (MGE) - associated proteins encoded by genes located in the same contigs as pdARDs. The 3.9 million gene catalogue results from a non-redundancy filtering at 95% for the genes[19], but in order to identify the contigs on which pdARDs were identified, we needed to return

to the redundant catalogue (*i.e.* the non-dereplicated catalogue of genes) and identified homologs sharing 95% nucleic acid identity with the pdARDs. By doing so, we could identify contigs (n=16,955) carrying at least one pdARD. The mean size of the contigs was 19,711 bp (min 500, max 461,981, median 8,513). In total, the 16,955 contigs contained a total of 908,888 genes after the subtraction of pdARDs. The 908,888 genes were then translated into proteins with Prodigal[42] and queried for IS elements using BLASTP (query size threshold 150 amino acids, e-value 1E-30, identity threshold 40%) against the ISfinder database[57]. Conjugative elements were queried among the same gene set (n=908,888) with Conjscan[58], using the default parameters and the filters recommended by the authors (best e-value<0.001 and sequence coverage of at least 50%). Most proteins belonging to the type IV secretion systems (T4SS), which are involved in conjugation, are ubiquitous in that they have numerous homologs. Hence, when searching for conjugation proteins in a 3.9 million protein catalogue, there would be a high risk of false positives. Accordingly, the colocation of hits was deemed crucial. A conjugative T4SS is made from:

- a protease (VirB4)
- a second coupling protein protease (t4cp)
- a relaxase (MOB)
- a proteic complex (MPF) composed of at least 10 proteins

In order to identify a T4SS on a contig, we required presence of at least 1 virB4 hit, a t4cp1 or t4cp2 hit, a MOB hit and a certain number of MPF hits. All hits must co-localize. A MOB element alone can mobilize a neighboring gene (such as an ARD-encoding gene) via other T4SSs. However, in our dataset the short length of contigs led us to adapt those parameters (following the recommendations of the developers of the Conjscan software). Besides the MOB element, we considered that the presence of 2 hits from the same family (e.g. T_virB6 and T_virB8, or B_traF and B_traH) or virB4+any hit from another family on the same contig as a pdARD was a strong indication of the presence of mobility associated elements. Integrons were identified using IntegronFinder[66] on the 16,955 contigs using default parameters.

We also searched for pdARDs in metagenomic species pan-genomes (MSPs)[26] obtained from the 9.9 million intestinal gene catalogue[27] using BLASTN with a 95% identity threshold over 90% of the query.

We also searched for homologs of pdARDs in Genbank with 97% identity threshold over 90% of the query. We found 820 out of 6095 pdARDs (13.5%) which aligned against 139,413 Genbank entries. We

filtered hits corresponding to a virus, a plasmid or a vague taxonomic affiliation by considering the following terms: “uncultured bacterium”, “artificial”, unidentified”, “uncultured organism”, “environmental samples” and “metagenome”.

Distribution of the pdARDs in the MetaHIT cohort (n=663 subjects)

pdARDs profiles were obtained from the abundance matrix of the 3.9 million genes as described in Nielsen *et al*[19]. The "reads per kilobase per million mapped reads" (RPKM) method was used to normalize the mapping counts. After summing the relative abundances of pdARDs genes belonging to the same family, Dirichlet multinomial mixture models were used to find ARDs clusters (*i.e.* resistotypes) using the Dirichlet Multinomial R package. The same method was applied to detect gut microbiota clusters *(i.e.* enterotypes)[59]. The Laplace criterion was used to define optimal number of clusters as described on oral and faecal microbial dataset[60]. By analogy with the term enterotype, we chose to name a cluster of subjects based on their similarity of their faecal relative abundance of pdARDs a “resistotype”. The Chi-squared test was used to assess the associations between resistotypes and enterotypes. Rarefaction analysis at one million reads was done to determine the gene richness per samples. RLQ analysis[61] was conducted to assess the associations between the relative abundances of pdARDs*,* their characteristics (family, size of the cluster of associated genes [CAG]) and those of subjects (enterotypes, resistotypes, gender, body mass index [BMI], age). Of note, we excluded the patients suffering from inflammatory bowel disorders from this analysis. Co-inertia analysis was conducted to assess the associations between microbiota beta-diversity and pdARDs profiles. Microbiota composition was assessed using metagenomics species (MGS, see below) relative abundance and beta-diversity by square root Jensen-Shannon Divergence (JSD). A principal coordinate analysis was done on JSD distance matrix and a principal component analysis was done on ARDs profiles. Both analyses were then subjected to co-inertia analysis and Monte-Carlo permutation was done to asses to robustness of shared inertia.

Constitution of cohorts of patients with various antibiotic exposures

We included three cohorts of patients with various exposures to antibiotics:

- Hospitalization without antibiotics: a total of 31 patients with no exposure to antibiotics or hospitalisation during the three preceding months and admitted to the medicine ward of the Beaujon University

Teaching Hospital (Clichy, France) were included and provided a faecal sample at admission. Among them, 16 also provided a stool sample at discharge. One patient received antibiotics between admission and discharge and was not further considered for the analysis. In total, 15 patients could provide a stool sample soon after admission (T0) and at discharge (T1). The mean time between T0 and T1 samples was 10.7 days. The mean age of patients was 67.8 years old and the gender ratio (M/F) was 1.3. All patients gave informed consent. This work was approved by the French National Institutional Review Board (IRB 00008522) and registered at clinicaltrials.gov (NCT02031588).

- Chronic exposure: 30 cystic fibrosis (CF) patients were enrolled at the Cystic Fibrosis Unit of the Ramón y Cajal Hospital in Madrid. One faecal sample was collected at the occasion of a consultation. All subjects for this study were provided a consent form describing the study and providing sufficient information for subjects to make an informed decision about their participation as faecal donors in this study. Cystic fibrosis is a genetic disease that leads to an impairment of the lung function through an uncontrolled production of mucus. The consequence is chronic bacterial colonization, resulting in deleterious reactive fibrosis of the lung. Bacterial load is controlled by chronic exposure to antibiotics (home-therapy, mostly oral and inhaled in our cohort), which has resulted in significant life prolongation, and the near-absence of hospital care. Hence, the CF patients had been exposed to various antibiotics during the five years before the faecal sample was collected:

  - Beta-lactams (ampicilln, amoxycillin, cloxacillin, piperacillin-tazobactam, cefepime, ceftriaxone, ceftazidime, cefditoren, meropenem): 25/30
  - Macrolides (azithromycin, clarithromcyin): 17/30
  - Colistin: 21/30
  - Fluoroquinolones (ciprofloxacin, levofloxacin, moxifloxacin): 26/30
  - Cotrimoxazole: 14/30
  - Glycopeptides (vancomycin): 1/30
  - Aminoglycosides (amikacin, tobramycin): 12/30
  - Tetracyclines (doxycycline, minocycline): 2/30
  - Linezolid: 3/30
  - Rifampin: 1/30
  - Fosfomycin: 5/30

On average, CF patients had been exposed to 5.9 different antibiotics and had an average of 12.2 antibiotic courses during the five years before the sample was taken. The mean age was 36.3 years old and the gender ratio (M/F) was 1.3. This protocol and any amendments were submitted to the Ethics Committee (EC) in agreement with local legal prescriptions, for formal approval of the study conduct. The consent form was obtained before that subject provided any faecal sample for the study and was signed by the subject or legally acceptable surrogate, and the investigator-designated research professional obtaining the consent. According to the National Spanish laws the study did not require the approval of the Ethics Committee. Nonetheless, the Ethics Committee of the Hospital Ramón y Cajal guaranteed that the study was performed done according to the good clinical practices guidelines.

- Short high dose exposure: selective digestive decontamination (SDD) consists in administering a mixture of topical and parenteral antibiotics and antifungal agents to a patient at admission in order to eliminate potential bacterial and fungal pathogens. SDD has been showed to significantly reduce mortality in the intensive care unit (ICU)[29] and is now part of standard care for intensive care patients in the Netherlands. To assess the effect of SDD on the intestinal microbiota, we analysed the faecal samples from 13 patients admitted to the ICU of the University Medical Centre of Utrecht (UMCU, Netherlands). The samples were collected at admission (T0, first sample passed after admission) and after SDD (T1). Among the 13 patients for whom a faecal sample could be obtained at T0, 10 could provide a faecal sample at T1. The mean age was 59.9 years old and the gender ratio (M/F) was 0.5. SDD consisted of 4 days of intravenous cefotaxime and topical application of tobramycin, colistin, and amphotericin B. Additionally, a subset of samples (n=4) from this cohort was cultured in a brain-heart infusion broth overnight in ambient atmosphere at 37°C. The protocol for the collection of stool samples was reviewed and approved by the institutional review board of the University Medical Centre of Utrecht (The Netherlands) under number 10/0225. Informed consent for faecal sampling during hospitalization was waived. Written consent was obtained for the collection of faecal samples after hospitalization.

Metagenomic sequencing and mapping.

Total faecal DNA was extracted[62,63] and sequenced using SOLiD 5500 wildfire (Life Technologies) resulting in a mean of 68.5 million sequences of 35-base-long single-end reads. High-quality reads were generated with quality score cut-off >20. Reads with a positive match with human, plant, cow or SOLiD adapter sequences were removed.

Filtered high-quality reads were mapped to the MetaHIT 3.9 million gene catalogue[19] using the METEOR software[64]. The read alignments were performed in colourspace with Bowtie software (version 1.1.0)[65]. Uniquely mapped reads (reads mapping to a single gene from the catalogue) were attributed to the corresponding genes. Shared reads (mapping different genes of the catalogue) were attributed according to the ratio of their unique mapping counts, as following: as a read can map on different genes of the catalogue, the abundance of a gene $G(A_g)$ depends on the abundance of uniquely mapped reads (A_u), *i.e.* reads that map only to the gene G, and on the abundance of N shared reads (A_s) that aligned with M genes in addition to the gene G:

$$A_g = A_u + A_s$$

where

$$A_s = \sum_{i=1}^{N} C_{o_i}$$

For each shared read, the gain of abundance corresponds to a coefficient C_o that takes in account the total number of uniquely mapped reads on the M genes:

$$C_{o_i} = \frac{A_u}{A_u + \sum_{j=1}^{M} A_{\mathrm{u_j}}}$$

For instance, if a gene G is mapped by 10 reads that only map to it (unique reads), but also with 1 read that also align on a gene M that was mapped by 5 unique reads, then:

$$A_g = 10 + \frac{10}{10+5} \approx 10.7$$

To decrease technical biases due to different sequencing depth, samples with at least 5 million mapped reads were downsized to 5 million mapped reads (random sampling of 5 million mapped reads without replacement) using R package momr[31]. The abundance of each gene in a sample was then normalized by dividing the number of reads that mapped to the gene (A_g) by the gene nucleotide length and by the total number of reads from the sample. The resulting set of gene abundances, termed a "microbial gene profile", was used to estimate the abundance of metagenomic species (MGS)[19].

Gene richness analysis

Microbial gene richness was calculated by counting the number of genes mapped at least once for a given sample. Gene richness was calculated using R package momr for samples where 5 million or more reads had been mapped to the 3.9 million gene catalogue.

MetaGenomic Species (MGS)

MGS are co-abundance gene groups with more than 700 genes and can be considered as part of complete bacterial species genomes. 741 MGS were delineated from 396 human gut microbiome samples[19]. In this study, the relative abundance of MGS was determined as the median abundance of 90% of the genes composing each cluster, meaning that the 10% genes with the lowest abundance for each MGS were not considered for the calculation of the abundance of the MGS. Typically, these genes correspond to genes with 0 count, to accessory genes (hence their detection is not constant) or to genes that are not detected because of insufficient sequencing depth. The MGS taxonomical annotation was updated by sequence similarity using NCBI BLASTN, when more than 50% of the genes matched the same reference of NCBI database (December 2014 version) at a threshold of 95% of identity and 90% of gene length coverage to get the species annotation[19].

Statistical analysis for the distribution of pdARDs and MGS between groups

Statistical analyses for the differential abundances of pdARDs and MGS were performed using the application SHAMAN[66] (http://shaman.c3bi.pasteur.fr/). Data are available at (https://github.com/aghozlane/evotar), with the graphical representations using the abundances from the matrix rarefied at 5M reads. The relationship between richness and the abundance of ARDs was assessed by Spearman correlation test. The statistical threshold for significance was set at a p-value of 0.05.

Data availability

The 6,095 pdARDs PDB files, nucleotide and amino acid sequences can be downloaded from http://mgps.eu/Mustard/. The 3.9 million gene catalogue and the metagenomic species database are accessible at https://www.cbs.dtu.dk/projects/CAG/. The reads from the clinical samples generated in this study are available under the accession number PRJEB27799 at the European Nucleotide Archive (ENA).

Code availability

The PCM code can be found at https://github.com/aghozlane/pcm.

References

1. Qin, J. *et al.* A human gut microbial gene catalogue established by metagenomic sequencing. *Nature* **464,** 59–65 (2010).
2. Ghosh, T. S., Gupta, S. S., Nair, G. B. & Mande, S. S. In silico analysis of antibiotic resistance genes in the gut microflora of individuals from diverse geographies and age-groups. *PloS One* **8,** e83823 (2013).
3. Hu, Y. *et al.* Metagenome-wide analysis of antibiotic resistance genes in a large cohort of human gut microbiota. *Nat. Commun.* **4,** 2151 (2013).
4. Forslund, K. *et al.* Country-specific antibiotic use practices impact the human gut resistome. *Genome Res.* **23,** 1163–1169 (2013).
5. Sommer, M. O. A., Dantas, G. & Church, G. M. Functional characterization of the antibiotic resistance reservoir in the human microflora. *Science* **325,** 1128–1131 (2009).
6. Moore, A. M. *et al.* Pediatric fecal microbiota harbor diverse and novel antibiotic resistance genes. *PloS One* **8,** e78822 (2013).
7. Gupta, S. K. *et al.* ARG-ANNOT, a new bioinformatic tool to discover antibiotic resistance genes in bacterial genomes. *Antimicrob. Agents Chemother.* **58,** 212–220 (2014).
8. McArthur, A. G. *et al.* The comprehensive antibiotic resistance database. *Antimicrob. Agents Chemother.* **57,** 3348–3357 (2013).
9. Zankari, E. *et al.* Identification of acquired antimicrobial resistance genes. *J. Antimicrob. Chemother.* **67,** 2640–2644 (2012).
10. Arango-Argoty, G. *et al.* DeepARG: a deep learning approach for predicting antibiotic resistance genes from metagenomic data. *Microbiome* **6,** 23 (2018).
11. Gibson, M. K., Forsberg, K. J. & Dantas, G. Improved annotation of antibiotic resistance determinants reveals microbial resistomes cluster by ecology. *ISME J.* **9,** 207–216 (2015).

12. Wright, G. D. The antibiotic resistome: the nexus of chemical and genetic diversity. *Nat. Rev. Microbiol.* **5,** 175–186 (2007).
13. Salyers, A. A., Gupta, A. & Wang, Y. Human intestinal bacteria as reservoirs for antibiotic resistance genes. *Trends Microbiol.* **12,** 412–416 (2004).
14. Ghosh, S., Sadowsky, M. J., Roberts, M. C., Gralnick, J. A. & LaPara, T. M. Sphingobacterium sp. strain PM2-P1-29 harbours a functional tet(X) gene encoding for the degradation of tetracycline. *J. Appl. Microbiol.* **106,** 1336–1342 (2009).
15. Stinear, T. P., Olden, D. C., Johnson, P. D., Davies, J. K. & Grayson, M. L. Enterococcal vanB resistance locus in anaerobic bacteria in human faeces. *Lancet* **357,** 855–856 (2001).
16. Penders, J., Stobberingh, E. E., Savelkoul, P. H. M. & Wolffs, P. F. G. The human microbiome as a reservoir of antimicrobial resistance. *Front. Microbiol.* **4,** (2013).
17. Zhang, Y. & Skolnick, J. TM-align: a protein structure alignment algorithm based on the TM-score. *Nucleic Acids Res.* **33,** 2302–2309 (2005).
18. Forsberg, K. J. *et al.* Bacterial phylogeny structures soil resistomes across habitats. *Nature* **509,** 612–616 (2014).
19. Nielsen, H. B. *et al.* Identification and assembly of genomes and genetic elements in complex metagenomic samples without using reference genomes. *Nat. Biotechnol.* **32,** 822–828 (2014).
20. Goossens, H., Ferech, M., Vander Stichele, R., Elseviers, M. & ESAC Project Group. Outpatient antibiotic use in Europe and association with resistance: a cross-national database study. *Lancet* **365,** 579–587 (2005).
21. Altschul, S. F., Gish, W., Miller, W., Myers, E. W. & Lipman, D. J. Basic local alignment search tool. *J. Mol. Biol.* **215,** 403–410 (1990).
22. Berglund, F. *et al.* Identification of 76 novel B1 metallo-β-lactamases through large-scale screening of genomic and metagenomic data. *Microbiome* **5,** (2017).
23. Everard, A. *et al.* Cross-talk between Akkermansia muciniphila and intestinal epithelium controls diet-induced obesity. *Proc. Natl. Acad. Sci. U. S. A.* **110,** 9066–9071 (2013).
24. Sokol, H. *et al.* Faecalibacterium prausnitzii is an anti-inflammatory commensal bacterium identified by gut microbiota analysis of Crohn disease patients. *Proc. Natl. Acad. Sci. U. S. A.* **105,** 16731–16736 (2008).

804 25. Leski, T. A. *et al.* Multidrug-resistant tet(X)-containing hospital isolates in Sierra Leone. *Int. J.*
805 *Antimicrob. Agents* **42,** 83–86 (2013).
806 26. Oñate, F. P. *et al.* MSPminer: abundance-based reconstitution of microbial pan-genomes from
807 shotgun metagenomic data. *bioRxiv* 173203 (2018). doi:10.1101/173203
808 27. Li, J. *et al.* An integrated catalog of reference genes in the human gut microbiome. *Nat.*
809 *Biotechnol.* **32,** 834–841 (2014).
810 28. Arumugam, M. *et al.* Enterotypes of the human gut microbiome. *Nature* **473,** 174–180 (2011).
811 29. de Smet, A. M. G. A. *et al.* Decontamination of the digestive tract and oropharynx in ICU patients.
812 *N. Engl. J. Med.* **360,** 20–31 (2009).
813 30. van Schaik, W. The human gut resistome. *Philos. Trans. R. Soc. Lond. B. Biol. Sci.* **370,** (2015).
814 31. Le Chatelier, E. *et al.* Richness of human gut microbiome correlates with metabolic markers.
815 *Nature* **500,** 541–546 (2013).
816 32. Pehrsson, E. C. *et al.* Interconnected microbiomes and resistomes in low-income human habitats.
817 *Nature* **533,** 212–216 (2016).
818 33. Léonard, F., Andremont, A., Leclerq, B., Labia, R. & Tancrède, C. Use of beta-lactamase-
819 producing anaerobes to prevent ceftriaxone from degrading intestinal resistance to colonization. *J.*
820 *Infect. Dis.* **160,** 274–280 (1989).
821 34. Bilinski, J. *et al.* Fecal Microbiota Transplantation in Patients with Blood Disorders Inhibits Gut
822 Colonization with Antibiotic-Resistant Bacteria: Results of a Prospective, Single-Center Study.
823 *Clin. Infect. Dis.* (2017). doi:10.1093/cid/cix252
824 35. Lupo, A., Coyne, S. & Berendonk, T. U. Origin and Evolution of Antibiotic Resistance: The
825 Common Mechanisms of Emergence and Spread in Water Bodies. *Front. Microbiol.* **3,** (2012).
826 36. Lagier, J.-C. *et al.* Culture of previously uncultured members of the human gut microbiota by
827 culturomics. *Nat. Microbiol.* **1,** 16203 (2016).
828 37. Illergård, K., Ardell, D. H. & Elofsson, A. Structure is three to ten times more conserved than
829 sequence--a study of structural response in protein cores. *Proteins* **77,** 499–508 (2009).
830 38. Baquero, F., Tedim, A. P. & Coque, T. M. Antibiotic resistance shaping multi-level population
831 biology of bacteria. *Front. Microbiol.* **4,** 15 (2013).
832 39. Martínez, J. L., Coque, T. M. & Baquero, F. What is a resistance gene? Ranking risk in
833 resistomes. *Nat. Rev. Microbiol.* **13,** 116–123 (2015).

40. Van Boeckel, T. P. *et al.* Global antibiotic consumption 2000 to 2010: an analysis of national pharmaceutical sales data. *Lancet Infect. Dis.* **14,** 742–750 (2014).
41. Allen, H. K., Moe, L. A., Rodbumrer, J., Gaarder, A. & Handelsman, J. Functional metagenomics reveals diverse beta-lactamases in a remote Alaskan soil. *ISME J.* **3,** 243–251 (2009).
42. Hyatt, D. *et al.* Prodigal: prokaryotic gene recognition and translation initiation site identification. *BMC Bioinformatics* **11,** 119 (2010).
43. Fu, L., Niu, B., Zhu, Z., Wu, S. & Li, W. CD-HIT: accelerated for clustering the next-generation sequencing data. *Bioinformatics* **28,** 3150–3152 (2012).
44. Powell, S. *et al.* eggNOG v3.0: orthologous groups covering 1133 organisms at 41 different taxonomic ranges. *Nucleic Acids Res.* **40,** D284-289 (2012).
45. Liu, Y.-Y. *et al.* Emergence of plasmid-mediated colistin resistance mechanism MCR-1 in animals and human beings in China: a microbiological and molecular biological study. *Lancet Infect. Dis.* **16,** 161–168 (2016).
46. Finn, R. D., Clements, J. & Eddy, S. R. HMMER web server: interactive sequence similarity searching. *Nucleic Acids Res.* **39,** W29-37 (2011).
47. Pearson, W. R. & Lipman, D. J. Improved tools for biological sequence comparison. *Proc. Natl. Acad. Sci. U. S. A.* **85,** 2444–2448 (1988).
48. Berman, H. M. *et al.* The Protein Data Bank. *Nucleic Acids Res.* **28,** 235–242 (2000).
49. Sievers, F. *et al.* Fast, scalable generation of high-quality protein multiple sequence alignments using Clustal Omega. *Mol. Syst. Biol.* **7,** 539 (2011).
50. Jones, D. T. Protein secondary structure prediction based on position-specific scoring matrices. *J. Mol. Biol.* **292,** 195–202 (1999).
51. Sali, A. & Blundell, T. L. Comparative protein modelling by satisfaction of spatial restraints. *J. Mol. Biol.* **234,** 779–815 (1993).
52. Wallner, B. & Elofsson, A. Can correct protein models be identified? *Protein Sci. Publ. Protein Soc.* **12,** 1073–1086 (2003).
53. Wiederstein, M. & Sippl, M. J. ProSA-web: interactive web service for the recognition of errors in three-dimensional structures of proteins. *Nucleic Acids Res.* **35,** W407-410 (2007).

862 54. Ortiz, A. R., Strauss, C. E. M. & Olmea, O. MAMMOTH (matching molecular models obtained
863 from theory): an automated method for model comparison. *Protein Sci. Publ. Protein Soc.* **11,**
864 2606–2621 (2002).
865 55. Tibshirani, R. Regression shrinkage and selection via the lasso. *J R. Stat. Soc B* **58,** 267–288
866 (1996).
867 56. Fan, R. E., Chang, K. W., Hsieh, C. J., Wang, X. R. & Lin, C. J. A library for large linear
868 classification. *JMLR* **9,** 1871–1874
869 57. Siguier, P., Perochon, J., Lestrade, L., Mahillon, J. & Chandler, M. ISfinder: the reference centre
870 for bacterial insertion sequences. *Nucleic Acids Res.* **34,** D32-36 (2006).
871 58. Guglielmini, J., Quintais, L., Garcillán-Barcia, M. P., de la Cruz, F. & Rocha, E. P. C. The
872 repertoire of ICE in prokaryotes underscores the unity, diversity, and ubiquity of conjugation. *PLoS*
873 *Genet.* **7,** e1002222 (2011).
874 59. Holmes, I., Harris, K. & Quince, C. Dirichlet multinomial mixtures: generative models for microbial
875 metagenomics. *PloS One* **7,** e30126 (2012).
876 60. Ding, T. & Schloss, P. D. Dynamics and associations of microbial community types across the
877 human body. *Nature* **509,** 357–360 (2014).
878 61. Dray, S. & Legendre, P. Testing the species traits-environment relationships: the fourth-corner
879 problem revisited. *Ecology* **89,** 3400–3412 (2008).
880 62. Godon, J. J., Zumstein, E., Dabert, P., Habouzit, F. & Moletta, R. Molecular microbial diversity of
881 an anaerobic digestor as determined by small-subunit rDNA sequence analysis. *Appl. Environ.*
882 *Microbiol.* **63,** 2802–2813 (1997).
883 63. Suau, A. *et al.* Direct analysis of genes encoding 16S rRNA from complex communities reveals
884 many novel molecular species within the human gut. *Appl. Environ. Microbiol.* **65,** 4799–4807
885 (1999).
886 64. Pons, N. *et al.* METEOR - a plateform for quantitative metagenomic profiling of complex
887 ecosystems. in (2010).
888 65. Langmead, B. & Salzberg, S. L. Fast gapped-read alignment with Bowtie 2. *Nat. Methods* **9,** 357–
889 359 (2012).
890 66. Quereda, J. J. *et al.* Bacteriocin from epidemic Listeria strains alters the host intestinal microbiota
891 to favor infection. *Proc. Natl. Acad. Sci. U. S. A.* **113,** 5706–5711 (2016).

892 67. Robert, P. & Escoufier, Y. A Unifying Tool for Linear Multivariate Statistical Methods: The RV-
893 Coefficient. *Appl. Stat.* **25,** 257 (1976).
894

Figures

Figure 1: Illustration of the concept of "Pairwise Comparative Modelling" (PCM) with a class A beta-lactamase (panel A). A1: class A beta-lactamase protein structure (4EWF) obtained from the PDB database. A2: A candidate protein (MC3.MG12.AS1.GP1.C14.G3 from *Faecalibacterium prausnitzii*) for class A beta-lactamase modelled with a reference class A beta-lactamase structural template. This protein had 26.5% amino acid identity with the closest reference class A beta-lactamase. A3: The same candidate protein (MC3.MG12.AS1.GP1.C14.G3) for class A beta-lactamase this time modelled with a negative reference template. The candidate MC3.MG12.AS1.GP1.C14.G3 was predicted to be a class A beta-lactamase with 100% confidence by our model and later found to be functional after gene synthesis. Panel B: Bar-plot of the activity of the synthesized pdARDs against antibiotics with respect to the degree of confidence of the prediction ("reference" meaning that the protein shares more ≥95% amino acid identity with a functionally proven ARD, "good" meaning a PCM score over 99% and a TmAlign Tm score ≥0.8, "fair" meaning a PCM score between 50% and 80%). Panel C: number of predictions of antibiotic resistance determinants from a 3.9 million gene catalogue of the intestinal microbiota[19] using PCM, BLASTP[21], ARG-ANNOT[7], Resfinder[9], DeepARG[10], Resfams[11] and the HMM-based method published by Berglund *et al*. for class B1 beta-lactamases[22]. Panel D: violin plot of the maximal identity observed with a reference ARD for candidates predicted as ARDs (blue violin, n=6,095) and those not predicted as ARDs (red violin, n=3,982). The point depicts the median. The width of the violins depicts the distribution of pdARDs according to their maximal identity with a reference ARD. See Supplementary Table 2 for details about candidates sharing at least 40% identity with reference ARDs but which were not predicted as ARDs.

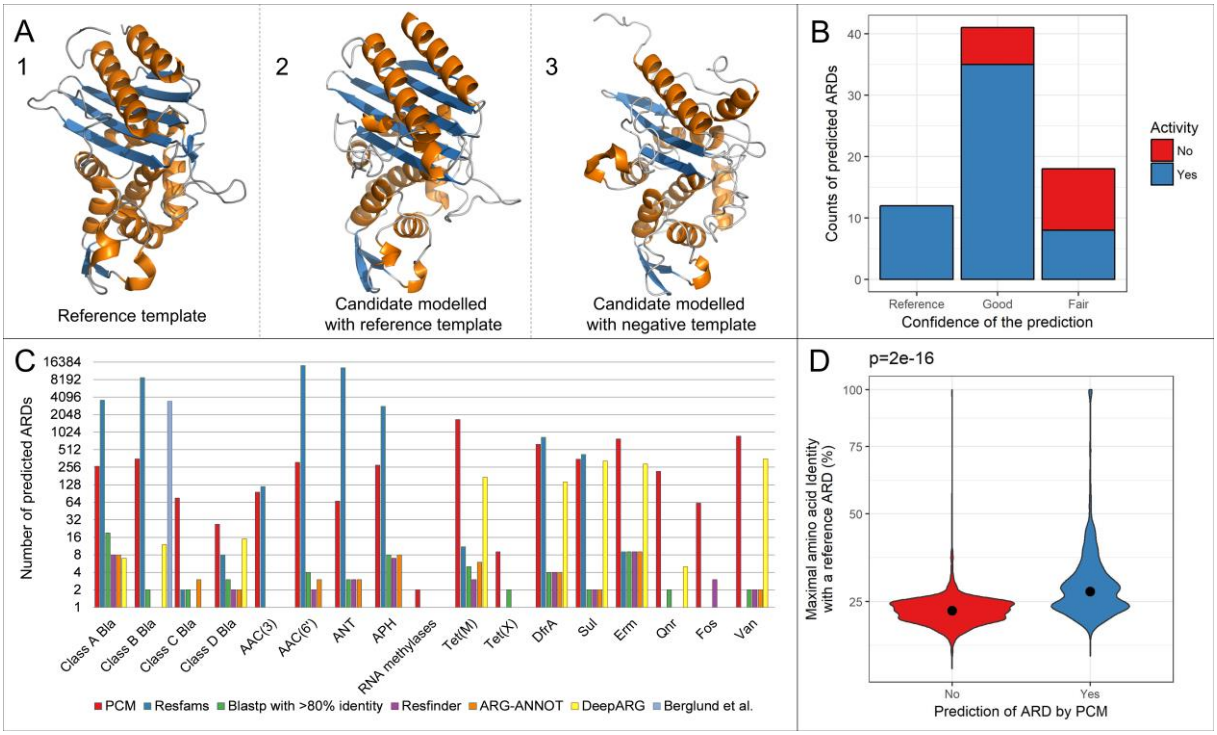

916

917 Bla: beta-lactamase; AAC: aminoglycoside acetylase; ANT: aminoglycoside nucleotidyl transferase;
918 APH: aminoglycoside phosphotransferase; DfrA: type A dihydrofolate reductase; Sul: dihydropteroate
919 synthase; Erm: erythromycin ribosome methylase; Qnr: quinolone resistance; Fos: fosfomycin
920 resistance (Fos); Van: D-Ala – D-Lac/Ser ligase (vancomycin resistance).

921

Figure 2: Mobile genetic elements (MGE) and predicted antibiotic resistance determinants (pdARDs). (A) Distribution of the sizes of the metagenomics unit (MGU) where an antibiotic resistance determinant was predicted with respect to the colocation of MGE-associated genes. The vertical line depicts the assumed gene size threshold above which MGUs are considered as partial chromosomes referred as metagenomic species (MGS)[19]. (B) Bar plot of the categories of metagenomic species pangenomes (MSPs)[26] assigned to MGE – associated genes[27] and pdARDs. (C) Proportion of pdARDs co-locating with MGE-associated genes with respect to their phylum. (D) Proportion of pdARDs co-locating with MGE-associated genes according to the pdARD family. Of note, the AAC(2') and 16S RNA methylases only included 3 and 2 pdARDs, respectively and were accordingly not depicted in this panel.

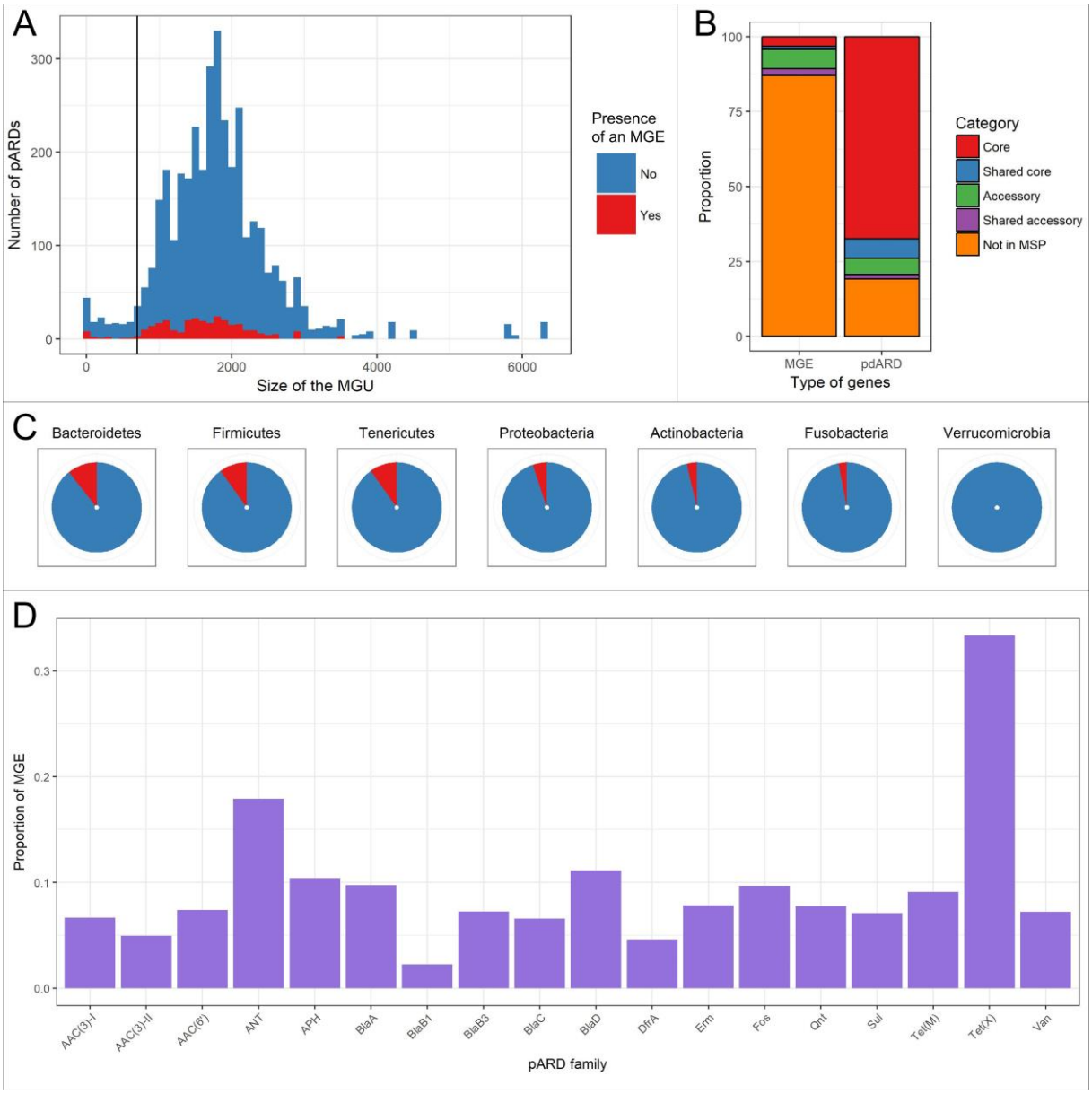

Figure 3: Association between resistotypes, enterotypes, metagenomics species (MGS) and pdARDs profiles in the 663 individuals from the MetaHIT cohort. A) inertia shared between pdARDs profiles and microbiota composition as function of bioinformatics methods. We assessed how gut microbiota beta diversity inertia was connected to the abundance of pdARDs. Co-inertia using RV coefficient was analysed to detect significant co-structure between datasets[67], meaning that different sets of variables (e.g. microbial genera abundance and ARDs profiles) were not independent and shared a fraction of inertia. Monte- Carlo tests were used to confirm observed relations between different datasets, assuming a p-value < 0.05. B) Samples proportions for each resistotype depicted as function of enterotypes using the PCM method. C) and D) Association between pdARDs gene profile and gut microbiota composition using co-inertia analysis with respect to their enterotypes and pdARDs families (C), and to their resistotypes and MGS relative abundance (D). A taxonomical correspondence for each MGS number can be found in the original paper[19]. Briefly, all MGS were Firmicutes with the exception of MGS:164 and MGS:445 (both Bacteroidetes).

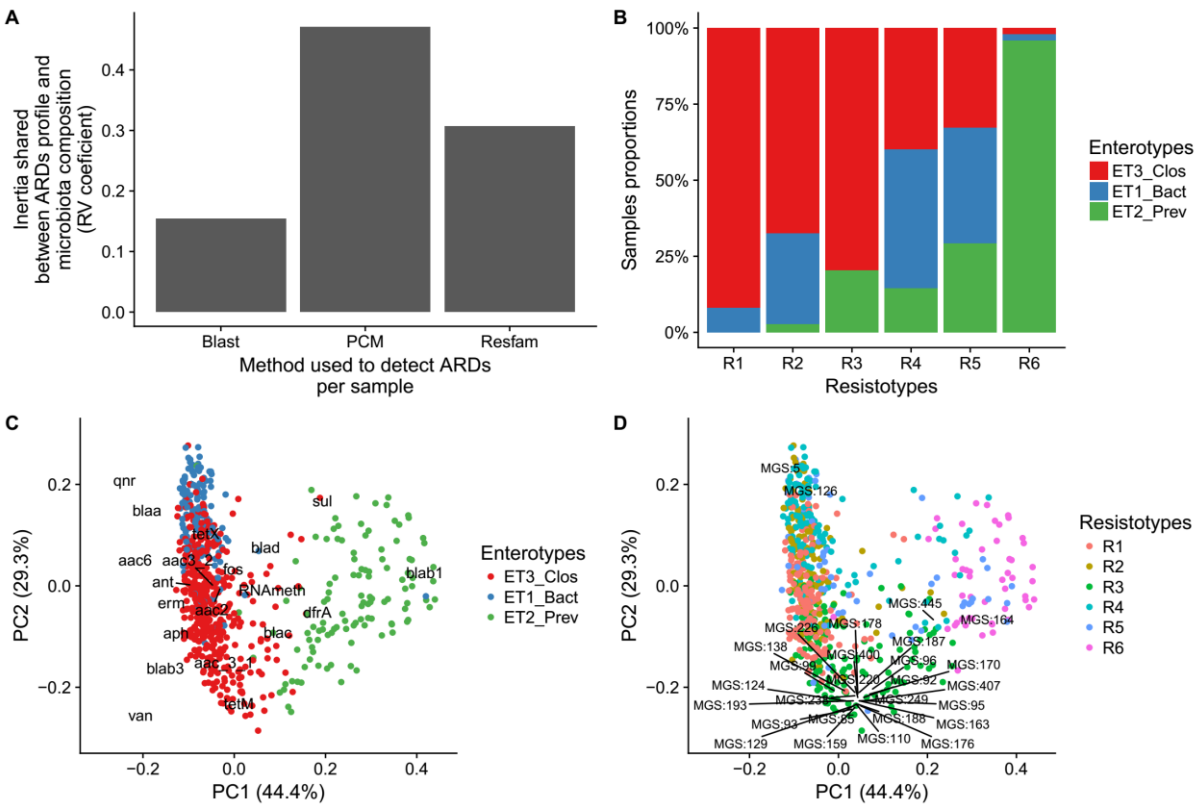

Figure 4: (A) Gene richness and relative abundance of predicted antibiotic resistance determinants (pdARDs) in the MetaHIT cohort (n=663). (B) Gene richness and relative abundance of pdARDs in our cohort of subjects with no recent antibiotic exposure (n=44). (C) Gene richness and relative abundance of pdARDs in our cohort of subjects with regards to their antibiotic exposure (n=102 samples). (D) and (E) Boxplots superimposed by dot plots of the comparisons of the relative abundance of all pdARDs and gene richness, respectively, between the various groups differing by their exposure to antibiotics. Hospitalization: n=15, Wilcoxon paired test. Short high dose exposure: n=10, Wilcoxon paired test. Chronic exposure: n=31 for patients not exposed to antibiotics, n=30 for patients chronically exposed to antibiotics, Wilcoxon unpaired test.

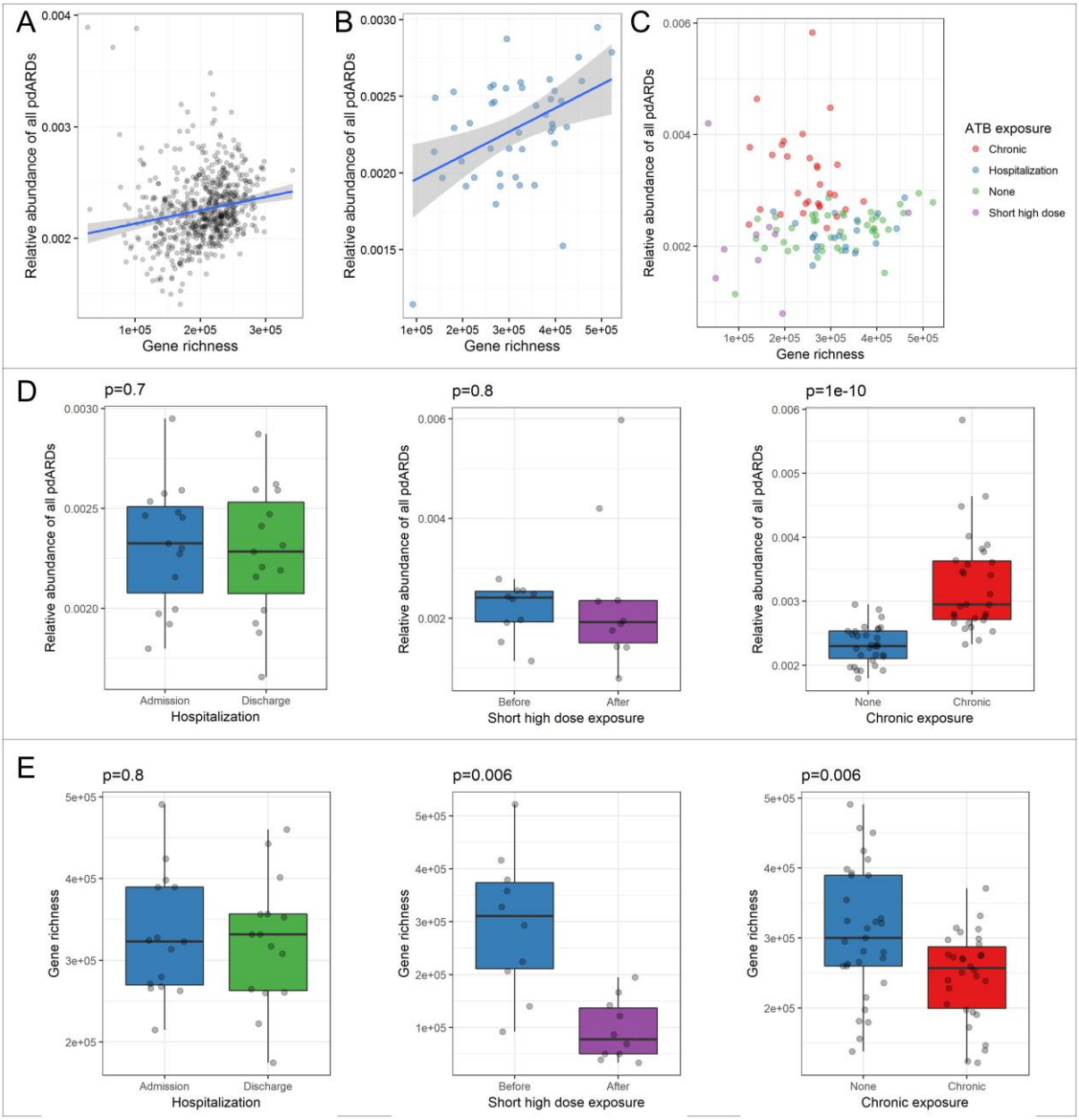

ATB: antibiotics. The shaded grey area depicts the 95% confidence interval around the blue, linear regression line. For boxplots, the lower, central and upper hinges correspond to the first, second (median) and third quartiles. The upper and lower whiskers respectively correspond to the higher and lower values at 1.5*IQR from the hinge (where IQR is the inter-quartile range, or distance between the first and third quartiles).

963 **Table 1**: Summary of the predictions of antibiotic resistance determinants (ARDs) from a 3.9 million
964 gene catalogue of the intestinal microbiota[19] and of gene synthesis results.

Antibiotic resistance class	Number of references	Number of candidates	Number of predictions	Rate ARD predictions/candidates (%)	Tested (%)	N functional (%)	N not functional (%)
16S rRNA methylase	17	4	2	50,0	0 (0%)	NA	NA
AAC(2')	5	15	3	20,0	0 (0%)	NA	NA
AAC(3)-I	7	53	15	28,3	2 (13.3%)	2 (100%)	0 (0%)
AAC(3)-II	12	81	81	100	5 (6.2%)	5 (100%)	0 (0%)
AAC(6')	36	1191	312	26,2	8 (2.6%)	6 (75%)	2 (25%)
ANT	29	158	67	42,4	3 (4.5%)	3 (100%)	0 (0%)
APH	30	430	279	64,9	4 (1.4%)	3 (75%)	1 (25%)
Class A beta-lactamase	682	402	267	66,4	14 (5.2%)	9 (64.3%)	5 (35.7%)
Class B1-B2 beta-lactamase	150	554	134	24,2	8 (6.0%)	6 (75%)	2 (25%)
Class B3 beta-lactamase	31	493	221	44,8	7 (3.2%)	5 (71.4%)	2 (28.6%)
Class C beta-lactamase	56	373	76	20,4	4 (5.3%)	4 (100%)	0 (0%)
Class D beta-lactamase	248	76	27	35,5	2 (7.4%)	2 (100%)	0 (0%)
DfrA	35	632	632	100	0 (0%)	NA	NA
Erm	58	873	781	89,5	0 (0%)	NA	NA
Fos	34	84	62	73,8	0 (0%)	NA	NA
Qnr	66	272	219	80,5	0 (0%)	NA	NA
Sul	33	357	353	98,9	0 (0%)	NA	NA
Tet(M)	72	2824	1682	59,6	13 (0.8%)	9 (69.2%)	4 (30.8%)
Tet(X)	12	42	9	21,4	1 (11.1%)	1 (100%)	0 (0%)
Van ligase	16	1163	873	75,1	0 (0%)	NA	NA

965